ACADEMIC PRESS

Available online at www.sciencedirect.com
SCIENCE DIRECT®

Journal of Solid State Chemistry 170 (2003) 265–272

JOURNAL OF SOLID STATE CHEMISTRY

http://elsevier.com/locate/jssc

Synthesis and crystal structure analysis of $Sr_8Cu_3In_4N_5$ and $Sr_{0.53}Ba_{0.47}CuN$

Hisanori Yamane,[a,*] Shinya Sasaki,[a] Shunichi Kubota,[a] Masahiko Shimada,[a] and Takashi Kajiwara[b]

[a] *Institute of Multidisciplinary Research for Advanced Materials, Tohoku University, 2-1-1 Katahira, Aoba-ku, Sendai 980-8577, Japan*
[b] *Department of Chemistry, Graduate School of Science, Tohoku University, Aramaki, Aoba-ku, Sendai 980-8578, Japan*

Received 27 June 2002; received in revised form 9 September 2002; accepted 17 September 2002

Abstract

Single crystals of new quaternary compounds $Sr_8Cu_3In_4N_5$ and $Sr_{0.53}Ba_{0.47}CuN$ were prepared, respectively, from a Sr–Cu–In–Na melt under 7 MPa of N_2 and from a Sr–Ba–Cu–In–Na melt under 0.5 MPa of N_2 by slow cooling from 1023 to 823 K. The crystal structures were determined by single-crystal X-ray diffraction. $Sr_8Cu_3In_4N_5$ has an orthorhombic structure (space group, *Immm*, $Z=2$, $a=3.8161(5)$ Å, $b=12.437(2)$ Å, $c=18.902(2)$ Å), and is isostructural with $Ba_8Cu_3In_4N_5$. It contains nitridocuprates of isolated units $^0[CuN_2]$ and one-dimensional linear chains $^1_\infty[CuN_{2/2}]$ and one-dimensional indium clusters $^1_\infty[In_2In_{2/2}]$. $Sr_{0.53}Ba_{0.47}CuN$ crystallizes in an orthorhombic cell, space group *Pbcm*, $Z=4$, $a=5.4763(7)$ Å, $b=9.2274(12)$ Å, $c=9.0772(12)$ Å. The structure contains infinite zig-zag chains $^1_\infty[CuN_{2/2}]$ which kink at every second nitrogen atom.

Keywords: Strontium copper nitride indium; Strontium barium copper nitride; Crystal structure; Single-crystal X-ray diffraction; Nitridocuprates; Zintl anion; Indium cluster

Introduction

In recent years, novel nitrides with alkaline-earth metal, transition metal, and post-transition metal elements have been synthesized using Na as a flux or reaction-enhanced media [1,2]. Various kinds of nitridometallate anions are contained in the structures. For the alkaline-earth metal copper nitrides, $Sr_6Cu_3N_5$, SrCuN, BaCuN, $Ba_{16}Cu_{13}N_{15}$ and $Ca_4BaCu_2N_4$ were prepared by the Na flux method and their crystal structures were determined by X-ray diffraction [3,4]. Isolated groups of $^0[CuN_2]$ or $^0[Cu_2N_3]$ and infinite bent or spiral chains of $^1_\infty[CuN_{2/2}]$ are contained in the structures. Recently, compounds $Ba_8Cu_3In_4N_5$ [5] and $Ba_{14}Cu_2In_4N_7$ [6] containing Zintl poly anions of indium in addition to the nitridocuprate groups were also prepared by the Na flux method. One-dimensional infinite $^1_\infty[In_2In_{2/2}]$ clusters, isolated groups $^0[CuN_2]$, and one-dimensional linear chains $^1_\infty[CuN_{2/2}]$ are included in $Ba_8Cu_3In_4N_5$. $Ba_{14}Cu_2In_4N_7$ contains $^0[CuN_2]$ groups and $^0[In_4]$ clusters.

In the crystal structure analysis of $Ba_8Cu_3In_4N_5$ [5], we adopted a split-site model for the arrangement of one-dimensional linear chains $^1_\infty[CuN_{2/2}]$ because of the large anisotropic displacement parameters of Cu and N atoms along the *a*-axis. The present study attempted to replace Ba with a smaller atom Sr and obtained single crystals of $Sr_8Cu_3In_4N_5$ for the study on the structure of the one-dimensional linear chains $^1_\infty[CuN_{2/2}]$. The crystal structure of a new nitride $Sr_{0.53}Ba_{0.47}CuN$ which was prepared during the experiments for the partial substitution of Ba with Sr was also reported.

Experimental

All materials were handled in an Ar-filled glove box (oxygen and moisture levels below 1 ppm). The elements utilized were Ba (99.99%, Aldrich), Sr (99%, Rare Metallic), Cu (99.99%, High Purity Chemical), In (99.999%, Rare Metallic) and Na (99.95%, Nippon

*Corresponding author. Fax: +81-22-217-5160.
E-mail address: yamane@tagen.tohoku.ac.jp (H. Yamane).

0022-4596/03/$ - see front matter © 2002 Elsevier Science (USA). All rights reserved.
doi:10.1016/S0022-4596(02)00083-X

Table 1
Sr ratio, s, in the starting melt (Sr:Ba:Cu:In:Na = s:2–s:1:1:6) and products prepared at P_{N_2} = 7 MPa and T = 1023 K

s	Product	Space group
0	$Ba_8Cu_3In_4N_5$	*Immm*
0.2	$(Sr,Ba)_8Cu_3In_4N_5$	*Immm*
0.6	(Sr,Ba)CuN	*Pbcm*
1.0	(Sr,Ba)CuN	*Pbcm*
1.5	(Sr,Ba)CuN	*Pnma*
2.0	$Sr_8Cu_3In_4N_5$	*Immm*

Soda). These metals were weighed with molar ratios (Sr: Ba:Cu:In:Na: = s:2−s:1:1:6) listed in Table 1 and loaded in a BN crucible (99.5%, Showadendo, inside diameter 7 mm, height 38 mm). The total amount of the starting materials was about 1 g. The crucible was placed into a stainless-steel container and sealed in the glove box. The details of the containers have been described elsewhere [7]. The container was connected to a N_2 gas feed line. After heating to 1023 K in an electric furnace, N_2 gas (>99.9999%, Nippon Sanso) or Ar (>99.9999%, Nippon Sanso) and N_2 gas was introduced into the container. The total pressure in the container was at 7 MPa. The sample was heated at this temperature for 1 h and then cooled from 1023 to 823 K at a rate of 2 K/h. Below 823 K, the sample was cooled to room temperature in the furnace by shutting off the electric power to the furnace. The products in the crucible were washed in liquid NH_3 (99.999%, Nippon Sanso) to dissolve away the Na flux. The details of the Na extraction procedure were described elsewhere [8].

The scanning electron microscope (SEM, Jeol ISM-5400F) equipped with an energy dispersive X-ray spectrometer (EDS, Voyger) was used to evaluate elemental compositions for Sr, Ba, In, and Cu. The samples ground in the glove box were sealed in thin-walled glass capillaries and characterized by X-ray powder diffraction on an imaging plate Gunier camera with Cu$K\alpha_1$ radiation (Huber 670). Single crystals were picked from the products, sealed in the glass capillaries, and checked by Laue and precession photographs for their singularity, lattice parameters, and symmetry. Diffraction data were collected on a single-crystal X-ray diffractometer with a two-dimensional CCD detector and graphite-monochromated Mo$K\alpha$ radiation (Bruker SMART System). The unit cells were refined during the integration with the program SAINT [9]. Face-indexed analytical absorption correction was applied to the collected diffraction intensity data with the program XPREP [10]. A structural model of $Sr_{0.53}Ba_{0.47}CuN$ was obtained by direct methods with the program SIR97 [11]. Refinement was performed using SHELXL97 [12].

Results and discussion

Synthesis

The compounds obtained from the products are shown in Table 1. The condition at $s = 0$ was for the synthesis of $Ba_8Cu_3In_4N_5$ reported in the previous paper [5].

Black metallic luster platelet single crystals (about 0.5 mm thick, 1.2 mm long) were grown at $s = 0.2$. The precession photographs indicated that the structure was the same as that of $Ba_8Cu_3In_4N_5$. The atomic ratio obtained from the EDX analysis was Sr:Ba:Cu:In = 0.5:7.6:2.9:4, which led to a formula of $Sr_{0.4}Ba_{7.6}Cu_3In_4N_5$. About 5% of Ba was substituted by Sr.

Prismatic crystals with black metallic luster were crystallized behind the crust of the sample prepared at $s = 0.6$ and 1.0. The maximum size of the crystals was $1.75 \times 0.25 \times 0.25$ mm. $BaIn_2$ and other unidentified substances, which were probably intermetallic compounds in the system of Ba, Sr, In, and Cu, were seen inside the crucible on the wall or bottom. Ba, Sr, and Cu were detected in the prismatic crystals, but indium was not found by EDX analysis. As described in the following section, the single crystals were $Sr_xBa_{1-x}CuN$ (orthorhombic, *Pbcm*). The metal ratios were Sr:Ba:Cu = 0.37–0.58:0.45–0.55:1 for the crystals picked up from the sample prepared at $s = 0.6$, and 0.31–0.49:0.70–0.76:1 at $s = 1.0$. The range of x is around from 0.3 to 0.6.

At $s = 1.5$, prismatic single crystals with a size less than $0.5 \times 0.5 \times 1.0$ mm were produced in the crucible with other small granular intermetallic compounds. The X-ray powder diffraction pattern of the crystals was similar to the calculated pattern of SrCuN [3] with the BaNiN-type structure (*Pnma*, $a = 9.045(2)$ Å, $b = 13.234(3)$ Å, $c = 5.388(1)$ Å). The lattice parameters of the crystals refined from the d-values of the indexed peaks were $a = 9.099(4)$ Å, $b = 13.2869(7)$ Å, and $c = 5.4105(3)$ Å. The EDX analysis showed the presence of Ba, Sr and Cu with the atomic ratio of 0.9:0.1 for Sr:Ba. The formula of the solid solution can be represented as $(Sr_{0.9}Ba_{0.1})CuN$.

The main products produced in the crucible at $s = 2.0$ were black fine-granule crystals of $Sr_8Cu_3In_4N_5$ with a size smaller than 0.1 mm. This would suggest very fast spontaneous nucleation in the melt. In order to decrease the number of nuclei in the melt, N_2 pressure was decreased from 7 to 0.5 MPa. When the sample was heated at 1023 K, 6.5 MPa of Ar gas was introduced first to reduce Na evaporation from the melt, and then N_2 gas was added up to the total pressure of 7 MPa. After slow cooling from this temperature, platelet single crystals of $Sr_8Cu_3In_4N_5$ with a size of about 1 mm were obtained.

The precession photographs confirmed that $Sr_8Cu_3In_4N_5$ has the space group *Immm*, the same as that of $Ba_8Cu_3In_4N_5$. The Sr:In:Cu molar ratio of the single crystals analyzed by EDX was 8:2.7–3.15:3.85–3.94, that was close to the ideal ratio of $Sr_8Cu_3In_4N_5$.

Electrical resistivity was measured for a single crystal of $Sr_8Cu_3In_4N_5$ with a size less than 2 mm in the elongated direction along the *a*-axis. The sample was sealed in a BN cell in which two In electrodes were attached. The resistivity at room temperature was 4.8 mΩ cm and decreased a little with decreasing temperature. The resistivity at 10–20 K was about 4.0 mΩ cm. Similar results were seen in the electrical properties of $Ba_8Cu_3In_4N_5$.

Since the single crystals prepared at $s=0.6$, 1.0 and 1.5 did not include In, we tried to prepare a sample from a starting metal mixture without In (Sr:Ba:Cu:Na = 1:1:1:6). The sample obtained by heating and cooling at the same conditions contained Ba_2N–Sr_2N powder and Cu metal. The melting point of Cu is 1358 K, but a liquid phase appears at 903 K at the composition Cu:In = 1:1 in the Cu–In binary system [13]. InN is unstable and decomposes into In metal and N_2 gas at the temperature and N_2 pressure of the synthesis in the present study [14]. Therefore, indium plays a role of flux which decreases the melting temperature of the metal mixture including Cu. SrCuN could not be synthesized with Cu metal [3]. The preparation of SrCuN was performed with Cu_3N. No BaCuN but $BaCu_{13}$ and unreacted Cu were obtained by using $BaN_{0.78}$ and Cu as starting materials. Niewa and DiSalvo used Cu_2O as a Cu source for BaCuN synthesis [4].

At or near the terminal compositions of $s=0$, 0.2 and 2.0, $Sr_xBa_{8-x}Cu_3In_4N_5$ and $Sr_8Cu_3In_4N_5$ were formed. However, the single crystals prepared at $s=0.6$–1.5 did not contain In. This might be explained by decreasing eutectic temperature in a multi-component system. Eutectic points at Ba- and Sr-rich compositions in Ba–In and Sr–In binary systems are 751 and 790 K, respectively [15]. In the systems of Ba–Sr–In or Ba–Sr–In–Cu, In would stay in the melt at lower temperature.

Crystal structure analysis

Details of the data collection and structure refinements are listed in Table 2. Positional along with equivalent isotropic displacement parameters, anisotropic displacement parameters, and important interatomic distances and bond angles are given in Tables 3, 4 and 5, respectively.

$Sr_8Cu_3In_4N_5$

This compound is isostructural with $Ba_8Cu_3In_4N_5$ and crystallizes in a body-centered orthorhombic cell, space group *Immm*. The lattice parameters of $Sr_8Cu_3In_4N_5$ ($a=3.8161(5)$ Å, $b=12.437(2)$ Å, and

Table 2
Crystal data and structure refinement for $Sr_8Cu_3In_4N_5$ and $Sr_{0.53}Ba_{0.47}CuN$

Formula	$Sr_8Cu_3In_4N_5$	$Sr_{0.53}Ba_{0.47}CuN$
Formula weight	1420.91	188.54
Crystal size (mm)	0.03 × 0.05 × 0.010	0.06 × 0.06 × 0.14
Crystal system, space group	Orthorhombic, *Immm*	Orthorhombic, *Pbcm*
Z	2	8
Temperature (K)	293(2)	293(2)
Unit-cell dimensions	$a=3.8161(5)$ Å	$a=5.4763(7)$ Å
	$b=12.437(2)$ Å	$b=9.2274(12)$ Å
	$c=18.902(2)$ Å	$c=9.0772(12)$ Å
Volume (Å^3)	897.1(2)	458.69(10)
Calculated density (Mg/m^3)	5.260	5.460
Absorption coefficient (mm^{-1})	32.049	29.181
θ range for data collection (deg)	1.96–30.03	4.33–29.98
Limiting indices	$-5\leqslant h\leqslant 5, -17\leqslant k\leqslant 17, -26\leqslant l\leqslant 26$	$-5\leqslant h\leqslant 7, -12\leqslant k\leqslant 12, -12\leq l<12$
Reflections collected/unique	5445/803 [R(int) = 0.1306]	3783/704 [R(int) = 0.0793]
Data/restrains/parameters	803/0/38	704/2/38
Goodness-of-fit on F^2, S	0.945	1.043
Final R indices [$l>2\sigma$ (I)]	$R_1=0.0366$, w$R_2=0.0769$	$R_1=0.0262$, w$R_2=0.0645$
R indices (all data)	$R_1=0.0466$, w$R_2=0.0798$	$R_1=0.0368$, w$R_2=0.0668$
Extinction coefficient	0.00047(7)	0.0007(3)
Largest diff. Peak and hole (e/Å^3)	1.666 and –1.918	1.278 and –1.308

$R_1=\sum \|\|F_o\|-|F_c\|\|/\sum F_o|$. w$R_2=\left[\sum w\,(F_o^2-F_c^2)^2/\sum (wF_o^2)^2\right]^{1/2}$, $w=1/\left[\sigma^2(F_o^2)+(aP)^2+bP\right]$, where F_o is the observed structure factor, F_c is the calculated structure factor, s is the standard deviation of F_c^2, and $P=[\mathrm{Max}(F_o^2,0)+2F_c^2]/3$ ($a=0.0343$, $b=0.000$ for $Sr_8Cu_3In_4N_5$, $a=0.0220$, $b=0.000$ for $Sr_{0.53}Ba_{0.47}CuN$). $S=\left[\sum w(F_o^2-F_c^2)^2/(n-p)\right]^{1/2}$, where n is the number of reflections and p is the total number of parameters refined.

Table 3
Atomic coordinates and isotropic displacement parameters for $Sr_8Cu_3In_4N_5$ and $Sr_{0.53}Ba_{0.47}CuN$

Atom	Site	Occupancy	x	y	z	U_{eq}[a]
$Sr_8Cu_3In_4N_5$						
Sr1	8*l*	1.0	1/2	0.35201(5)	0.21071(3)	0.0099(2)
Sr2	8*l*	1.0	1/2	0.34742(6)	0.40179(3)	0.0099(2)
In1	4*h*	1.0	1/2	0.64905(7)	0	0.0293(2)
In2	4*j*	1.0	0	1/2	0.08264(4)	0.0245(2)
Cu1	4*j*	1.0	1/2	0	0.19238(6)	0.0101(2)
Cu2	2*b*	1.0	1/2	0	0	0.0113(3)
Nl	8*l*	1.0	0	0.3480(5)	0.3057(3)	0.0117(11)
N2	2*a*	1.0	0	0	0	0.014(2)
$Sr_{0.53}Ba_{0.47}CuN$						
Sr1/Ba1	4*d*	0.703(8)/0.297 (8)	0.24868/(11)	0.43263(6)	1/4	0.0100(2)
Sr2/Ba2	4*c*	0.365(9)/0.635(9)	0.72250(9)	1/4	0	0.0098(2)
Cu	8*e*	1.0	0.23531(12)	0.08958(7)	0.11379(7)	0.0112(2)
N1	4*d*	1.0	0.4637(12)	0.1695(7)	1/4	0.0109(13)
N2	4*a*	1.0	0	0	0	0.0165(14)

[a] The equivalent isotropic displacement parameter, U_{eq} in Å^2, is defined as one-third of the trace of the orthogonalized U_{ij} tensor.

Table 4
Anisotropic displacement parameters (Å^2) for $Sr_8Cu_3In_4N_5$ and $Sr_{0.53}Ba_{0.47}CuN$

Atom	U_{11}	U_{22}	U_{33}	U_{23}	U_{13}	U_{12}
$Sr_8Cu_3In_4N_5$						
Sr1	0.0086(3)	0.0106(3)	0.0106(3)	0.0002(2)	0	0
Sr2	0.0083(3)	0.0172(4)	0.0102(3)	−0.0021(2)	0	0
Inl	0.0359(5)	0.0257(5)	0.0265(5)	0	0	0
In2	0.0282(4)	0.0315(5)	0.0137(4)	0	0	0
Cu1	0.0090(5)	0.0094(6)	0.0120(6)	0	0	0
Cu2	0.0051(7)	0.0154(9)	0.0133(8)	0	0	0
Nl	0.011(3)	0.011(3)	0.013(3)	−0.0023(19)	0	0
N2	0.004(5)	0.024(7)	0.015(6)	0	0	0
$Sr_{0.53}Ba_{0.47}CuN$						
Srl/Bal	0.0107(3)	0.0094(3)	0.0098(3)	0	0	0.0011(2)
Sr2/Ba2	0.0092(3)	0.0092(3)	0.0110(3)	0.0017(2)	0	0
Cu	0.0094(4)	0.0143(4)	0.0099(3)	−0.0019(2)	−0.0007(2)	−0.0035(2)
Nl	0.007(3)	0.018(4)	0.008(3)	0	0	−0.005(2)
N2	0.015(3)	0.020(4)	0.014(3)	−0.004(3)	−0.001(3)	−0.006(2)

The anisotropic displacement factor exponent takes the form: $-2\pi^2[h^2a^{*2}U_{11}+\cdots+2hk\ a^*b^*U_{12}]$.

$c = 18.902(2)$ Å) are 0.26 Å (6.4%) for the a-axis, 0.15 Å (1.2%) for the b-axis, and 0.9 Å (4.6%) for the c-axis smaller than those of $Ba_8Cu_3In_4N_5$.

The structure was refined with R_1 of 4.66% and wR_2 of 7.98% for all data. Fig. 1 illustrates the crystal structure of $Sr_8Cu_3In_4N_5$. The Cu1 atoms are almost linearly coordinated to two N atoms (<N1–Cu1–N1 = 177.8(3)°) with a Cu1–N1 interatomic distance of 1.890(6) Å. The angle and length are identical with 177.2(6)° and 1.880(7) Å of $Ba_8Cu_3In_4N_5$ within the standard deviations.

Linear infinite chains of [–Cu2–N2–] run along the a-axis. A split-site model was applied for the arrangement of [–Cu2–N2–] chains in the structure analysis of $Ba_8Cu_3In_4N_5$ because the anisotropic displacement parameters of U_{11} for Cu2 and N2 atoms were very large without splitting sites [5]. However, such anomalies of the displacement parameters were not seen in $Sr_8Cu_3In_4N_5$. The Cu2–N2 distance of 1.9080(2) Å in the chain of $Sr_8Cu_3In_4N_5$ is comparable with the Cu–N distances (1.87–1.90 Å) observed in the infinite chains and isolate units of nitrides such as $Sr_6Cu_2N_5$, SrCuN, BaCuN, and $Ba_{16}Cu_{13}N_{15}$ [3,4].

N1 atom is coordinated to one Cu atom and five Sr atoms, in Cu1 $(Sr1)_3(Sr2)_2$ octahedron. N2 atom is coordinated to two Cu atoms and four Sr atoms, in $(Cu2)_2$ $(Sr2)_4$ octahedron. N1–Sr1, N1–Sr2, and N2–Sr2 distances (2.507(6)–2.6547(7) Å) are consistent with those reported for SrCuN, $Sr_{39}Co_{12}N_{31}$, and SrNiN (2.45–2.89 Å) [3, 8, 16]. Similar as in the structure of

Table 5
Selected interatomic distances (Å) and bond angles (deg) for $Sr_8Cu_3In_4N_5$ and $Sr_{0.53}Ba_{0.47}CuN$

$Sr_8Cu_3In_4N_5$		$Sr_{0.53}Ba_{0.47}CuN$	
Nl–Cul	1.890(6)	Nl–Cul × 2	1.907(5)
–Sr1	2.507(6)	–Sr1/Ba1	2.694(7)
–Srl × 2	2.621(4)	–Srl/Ba1	2.699(7)
–Sr2 × 2	2.634(4)	–Sr2/Ba2 × 2	2.777(4)
N2–Cu2 × 2	1.9080(2)	N2–Cu × 2	1.8468(6)
–Sr2 × 4	2.6547(7)	–Sr1/Ba1 × 2	2.7186(4)
In1–In2 × 4	3.0849(8)	–Sr2/Ba2 × 2	2.7624(4)
–Inl	3.707(2)	Cu–Cu	2.4728(13)
–Sr2 × 4	3.6295(9)		
In2–Inl × 4	3.0849(8)	N1–Cu–N2	173.37(14)
–In2	2.124(2)	Cu–N1–Cu	80.8(2)
–Srl × 4	3.5900(8)	Cu–N2–Cu	180
N1–Cu1–N1	177.8(3)		
N2–Cu2–N2	180		
Cu2–N2–Cu2	180		

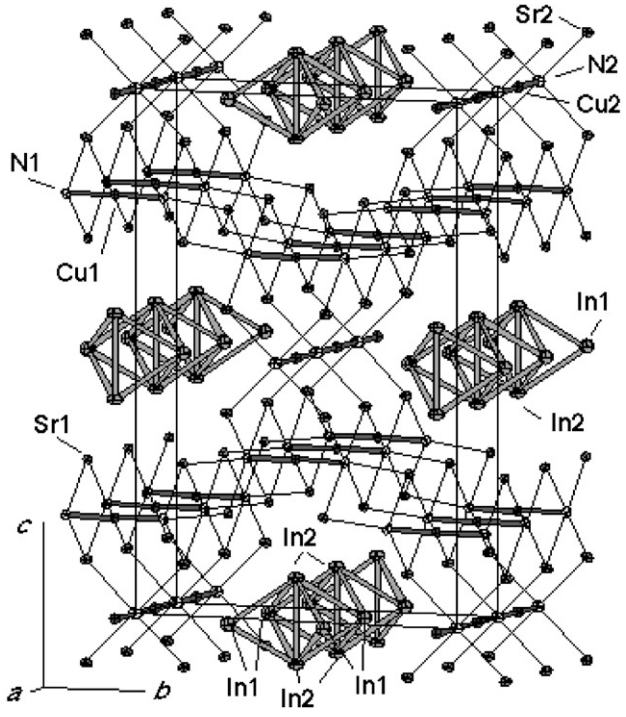

Fig. 1. The crystal structure of $Sr_8Cu_3In_4N_5$ with 50% probability displacement ellipsoids.

$Ba_8Cu_3In_4N_5$ [5], these nitrogen-centered metal octahedra continue and form channels along the *a*-axis by sharing edges and corners of the octahedra. One-dimensional infinite indium clusters $^1_\infty[In_2In_{4/2}]$ are included in the tunnels. The distances between In and Sr atoms are 3.6295(9) Å for In1–Sr2, and 3.5900(8) Å for In2–Sr1. The values are in the range of In–Sr distances (2.51–3.84 Å) reported for Sr_4In_2N [17] in which one-dimensional zig-zag chains $^1_\infty[In]$ are included.

In the previous study [5], the formal valences of the atoms in $Ba_8Cu_3In_4N_5$ were discussed and the compound was represented as $(Ba^{2+})_8$ $(^0[CuN_2]^{5-})_2$ $(^1_\infty[CuN^{2-}_{2/2}])$ $(^1_\infty[In_2In^{4-}_{4/2}])$. Following this form, $Sr_8Cu_3In_4N_5$ can also be represented as $(Sr^{2+})_8$ $(^0[CuN_2]^{5-})_2$ $(^1_\infty[CuN^{2-}_{2/2}])$ $(^1_\infty[In_2In^{4-}_{4/2}])$.

The unit length of the infinite clusters $^1_\infty[In_2In_{4/2}]$ that equals to the *a*-axis length becomes 0.26 Å (6.4%) smaller by substitution of Sr for Ba. The length of four equivalent bonding between In1 and In2 atoms (3.0849(8) Å) is slightly larger than the length in $Ba_8Cu_3In_4N_5$ (3.0655(8) Å). On the other hand, the distance of In1–In1 along the *b*-axis in $Sr_8Cu_3In_4N_5$ (3.707(2) Å) is 0.41 Å (12%) larger than the distance in $Ba_8Cu_3In_4N_5$ (3.298(2) Å). This reflects only a slight decrease of the *b*-axis length by Sr substitution. In2–In2 distance along the *c*-axis in $Sr_8Cu_3In_4N_5$ (3.124(2) Å) is only 0.05 Å smaller than that in $Ba_8Cu_3In_4N_5$ (3.175(2) Å). The increase of In1–In1 length along the *b*-axis may compensate the decreases of In–In bond lengths in the directions of other axes, in particular along the *a*-axis.

$Sr_{0.53}$ $Ba_{0.47}CuN$

The crystal used for structure determination was picked up from the product obtained at $s = 1.0$. Two possible space groups $Pbc2_1$ and *Pbcm* are consistent with the observed systematic extinctions. A crystal structure model was obtained with *Pbcm*. The final anisotropic refinement converged at $R_1 = 3.68\%$ and $wR_2 = 6.45\%$ for all data. The occupancies of Sr and Ba atoms in Sr1/Ba1 and Sr2/Ba2 sites were refined to be 0.703(8)/0.297(8) and 0.365(9)/0.635(9), respectively. This result gave the composition of $Sr_{0.53}Ba_{0.47}CuN$ for this crystal. The molar ratio of Sr:Ba:Cu was in the range of the ratios (Sr:Ba:Cu = 0.37–0.58:0.45–0.55:1) analyzed by EDX for the crystals in the sample.

Fig. 2 shows the crystal structure of $Sr_{0.53}Ba_{0.47}CuN$. The structure is characterized by zig-zag infinite chains of $^1_\infty[CuN_{1/1}]$ which kink at every second nitrogen atom (N2) and run along the *c*-axis. The structure of the chains is projected on the *a*–*b* plane in Fig. 3. The Cu and N atoms of the zig-zag chains are almost on the same plane close to (310) or $(\bar{3}10)$.

Similar bent Cu–N infinite chains were reported for SrCuN and BaCuN. Fig. 4 compares the sequence of the bent $^1_\infty[CuN_{1/1}]$ chains. The chains kink every third nitrogen atom in SrCuN, and alternately at the first and then the second nitrogen atom in BaCuN. The Cu–N distances of 1.8468(6) and 1.907(5) Å in $Sr_{0.53}Ba_{0.47}CuN$ are comparable with those in SrCuN (1.858–1.883 Å) and BaCuN (1.856–1.89 Å). In these three nitrides, the Cu–N–Cu angles at the bend positions are less than 90°, from 80.8° to 82.4°. Cu–Cu distances are in the range 2.473–2.49 Å, and shorter than that in copper metal (2.55 Å) [18]. The formal charge of Cu in $Sr_{0.53}Ba_{0.47}CuN$,

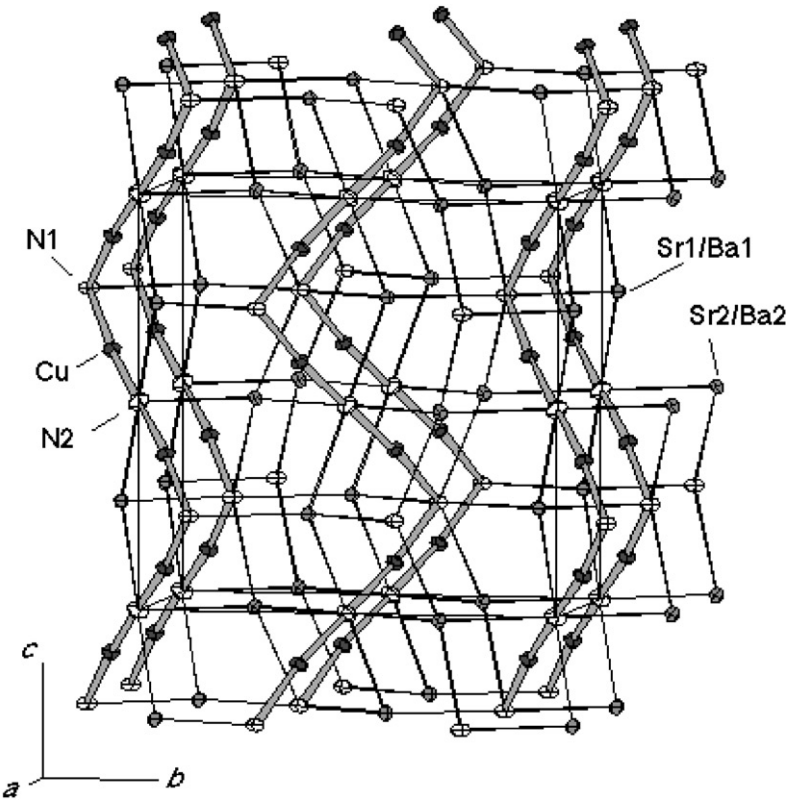

Fig. 2. The crystal structure of $Sr_{0.53}Ba_{0.47}CuN$ with 50% probability displacement ellipsoids.

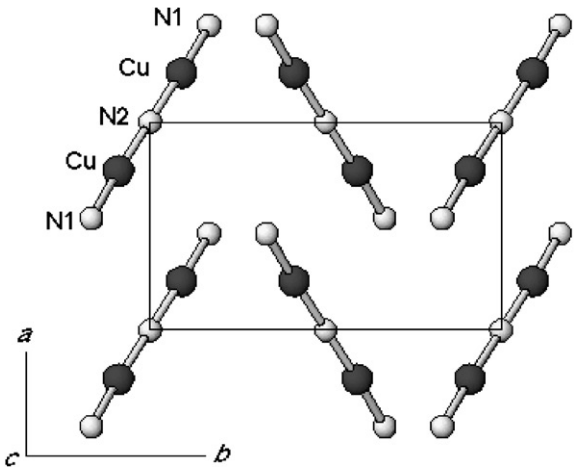

Fig. 3. Arrangement of $^{1}_{\infty}[CuN_{2/2}]$ zig-zag chains in $Sr_{0.53}Ba_{0.47}CuN$ projected on the a–b plane.

as well as in SrCuN and BaCuN, is regarded to be +1. $Sr_{0.53}Ba_{0.47}CuN$ is represented as $(Sr_{0.53}Ba^{2+}_{0.47})\,^{1}_{\infty}[CuN^{2-}_{1/1}]$.

The bent Cu–N infinite chains in the structure of SrCuN (*Pnma* $a=9.045(2)$ Å, $b=13.234(3)$ Å, $c=5.388(1)$ Å [3]) run along the c'-axis in another axis setting of the unit cell ($a'=5.388(1)$ Å, $b'=9.045(2)$ Å, $c'=13.234(3)$ Å) with the same symmetry of space group *Pbnm* ($P2_1/b\ 2_1/n\ 2_1/m$). The space group *Pbnm* is non-isomorphic subgroup of the space group *Pbcm* ($P2/b\ 2_1/c\ 2_1/m$). Thus, the structure of $Sr_{0.53}Ba_{0.47}CuN$ can be shown with the subgroup by taking the length of the a-axis two times longer than the original one and by replacing two-fold axes along the a-axis direction with screw axes. Although the periods of the bent in the Cu–N chains are different (13.234(3) Å for SrCuN and 9.0772(12) Å for $Sr_{0.53}Ba_{0.47}CuN$), atoms in both chains align with the same symmetry $2_1/m$ along the c' and c-axis.

The Sr1/Ba1 site with a larger Sr occupation is wedged in the V-shaped [–Cu–N–] chains of $Sr_{0.53}Ba_{0.47}CuN$.

The occupancy of Ba is larger than that of Sr in Sr2/Ba2 site which is situated outside the chains. The distances of Sr1/Ba1–N (2.694(7)–2.7186(4) Å) and Sr2/Ba2–N (2.7624(4)–2.777(4) Å) in $Sr_{0.53}Ba_{0.47}CuN$ are in the range of Sr–N and Ba–N distances in SrCuN (2.640–2.708 Å), in $Sr_6Cu_3N_5$ (2.60–2.94 Å), and in BaCuN (2.78–2.97 Å).

N1 and N2 atoms are coordinated to two Cu, two Ba1/Sr1 and two Sr2/Ba2 atoms (six metal atoms in total). Fig. 5 illustrates the crystal structure with the nitrogen-centered metal octahedra. Each N1–Cu_2(Sr, $Ba)_4$ and N2–Cu_2(Sr,$Ba)_4$ octahedra form layers in the b–c plane by sharing corners. These layers stack alternately along the a-axis by sharing the corners and edges of the metal octahedra.

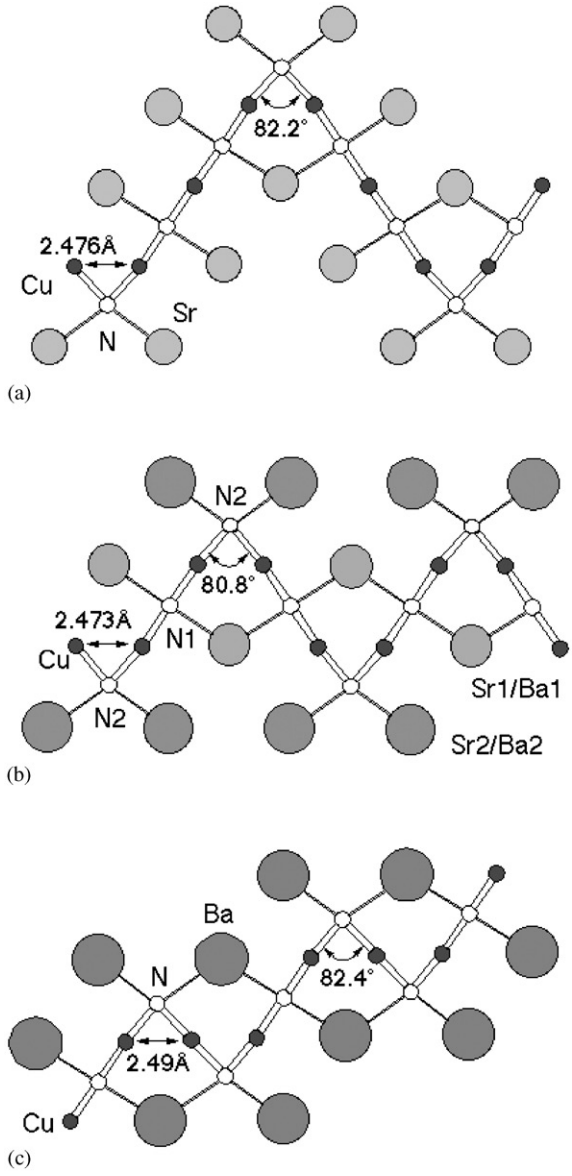

Fig. 4. Comparison of $^{1}_{\infty}[CuN_{2/2}]$ zig-zag chains in the structures of SrCuN (a), $Sr_{0.53}Ba_{0.47}CuN$ (b), and BaCuN (c).

As shown in Fig. 4, alkaline-earth nitridocuprates except CaCuN have one-dimensional infinite zig-zag chains $^{1}_{\infty}[CuN_{1/1}]$. CaCuN is composed of one-dimensional linear chains of $^{1}_{\infty}[CuN_{1/1}]$ [4,19]. Ca atoms are situated around the linear chains. The bent structures are probably introduced to eliminate the size mismatch between the $^{1}_{\infty}[CuN_{1/1}]$ chain and large alkaline-earth atoms of Sr and/or Ba. The periods of the repeated units in the zig-zag $^{1}_{\infty}[CuN_{1/1}]$ chains are three of the [N–Cu–N] unit for BaCuN, four for $Sr_{0.53}Ba_{0.47}CuN$, and six for SrCuN. The periods increase with decreasing size of alkaline-earth atoms.

The infinite chains $^{1}_{\infty}[CuN_{1/1}]$ are linear in $Ba_8Cu_3In_4N_5$ and $Sr_8Cu_3In_4N_5$ although the chains are surrounded by Ba or Sr atoms. This is probably due to the presence of one-dimensional infinite indium clusters $^{1}_{\infty}[In_2In_{4/2}]$ which run in the same direction of the linear $^{1}_{\infty}[CuN_{1/1}]$ chain. However, the large displacement of Cu and N atoms from the ideal positions were recognized and the split-site model was applied in the structure analysis of $Ba_8Cu_3In_4N_5$. This suggests the inherent Cu–N distance is kept locally in the [–Cu–N–] chain structure of $Ba_8Cu_3In_4N_5$. Such anomaly is not observed in the analysis of $Sr_8Cu_3In_4N_5$. Instead of the site splitting or anomalous anisotropic displacement parameters of Cu and N in the infinite chains, the $^{1}_{\infty}[In_2In_{4/2}]$ clusters are compressed along the direction of the chains and deformed due to the substitution of Ba atoms with the smaller Sr atoms. Combinations of nitridometallate anions and Zintl poly-anions may bring much more variations in the structures of nitride-related compounds.

Acknowledgments

We would like to thank Professor T. Ito for his encouragement and support and Y. Hayasaka for the EDX analysis. This work was supported in part by the

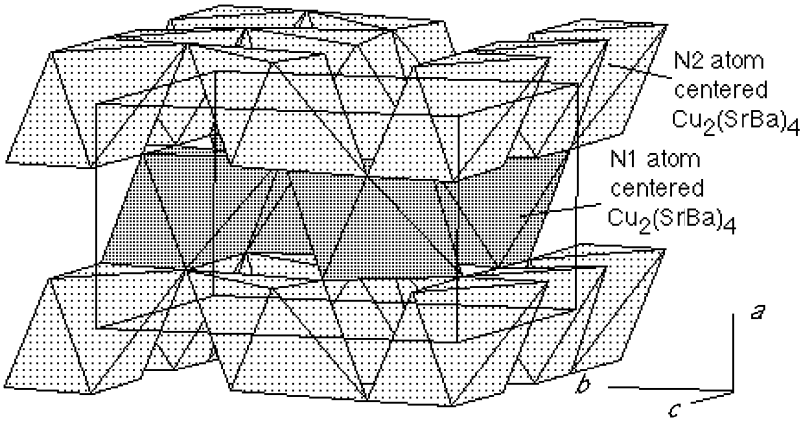

Fig. 5. The crystal structure of $Sr_{0.53}Ba_{0.47}CuN$ in a representation using nitrogen-centered $Cu_2(Sr/Ba)_4$ octahedra.

grant from Ministry of Education, Culture, Sports, Science and Technology.

References

[1] F.J. DiSalvo, S.J. Clarke, Curr. Opin. Solid State Mater. Sci. 1 (1996) 241.
[2] R. Niewa, F.J. DiSalvo, Chem. Mater. 10 (1998) 2733.
[3] F.J. DiSalvo, S.S. Trail, H. Yamane, N.E. Brese, J. Alloys Compd. 255 (1997) 122.
[4] R. Niewa, F.J. DiSalvo, J. Alloys Compd. 279 (1998) 153.
[5] H. Yamane, S. Sasaki, S. Kubota, R. Inoue, M. Shimada, T. Kajiwara, Solid State Chem. 163 (2002) 449 (doi:10.1006/jssc.2001.9424).
[6] H. Yamane, S. Sasaki, S. Kubota, T. Kajiwara, M. Shimada, Acta Crystallogr. C 58 (2002) i50.
[7] M. Aoki, H. Yamane, M. Shimada, T. Sekiguchi, T. Hanada, T. Yao, S. Sarayama, F.J. DiSalvo, J. Crystal Growth 218 (2000) 7.
[8] G.R. Kowach, H.Y. Lin, F.J. DiSalvo, J. Solid State Chem. 141 (1998) 1 (SC987850).
[9] Bruker, SAINT, Bruker AXS Inc. Madison, WI, USA, 1999.
[10] Bruker, XPREP, Bruker AXS Inc. Madison, WI, USA, 1997.
[11] A. Altomare, M.C. Burla, M. Camalli, G.L. Cascarano, C. Giacovazzo, A. Guagliardi, A.G.G. Molterni, G. Polidori, R. Spagna, J. Appl. Crystallogr. 32 (1999) 115.
[12] G.M. Sheldrick, SHELXL97, University of Göttingen, Germany, 1997.
[13] H. Okamoto, J. Phase Equilibria 15 (1994) 226.
[14] P. Porowski, I. Grzegory, J. Crystal Growth 178 (1997) 174.
[15] H. Okamoto, in: C.E.T. White, H. Okamoto (Eds.) Phase Diagrams of Indium Alloys and their Engineering Applications, ASM International, Materials Park, OH, 1992, pp. 42–43 (for Ba–In), pp. 258–259 (for Sr–In).
[16] T. Yamamoto, S. Kikkawa, F. Kanamaru, J. Solid State Chem. 115 (1995) 353.
[17] G. Cordier, S. Rönninger, Z. Naturforsch. 42b (1987) 825.
[18] I.-K. Suh, H. Ohta, Y. Waseda, J. Mater. Sci. 23 (1988) 757.
[19] J. Jäger, Ph.D. Thesis. Technische Hochshule Darmstadt, 1995.